

Oxidized $\text{Al}_x\text{Ga}_{1-x}\text{As}$ heterostructure planar waveguides

Y. Luo,^{a)} D. C. Hall, and L. Kou

Department of Electrical Engineering, University of Notre Dame, Notre Dame, Indiana 46556-5637

L. Steingart and J. H. Jackson

Metricon Corporation, P.O. Box 63, Pennington, New Jersey 08534

O. Blum and H. Hou^{b)}

Sandia National Laboratory, P.O. Box 0603, Albuquerque, New Mexico 87185-0603

(Received 30 July 1999; accepted for publication 20 September 1999)

Waveguiding by total internal reflection is demonstrated within $\text{Al}_x\text{Ga}_{1-x}\text{As}$ semiconductor heterostructures which have been fully oxidized in water vapor at $\sim 490^\circ\text{C}$. Refractive index, mode propagation constant, propagation loss ($\leq 3\text{ cm}^{-1}$) at $\lambda_0 = 1.3$ and $1.55\ \mu\text{m}$, secondary ion mass spectrometry depth profile, and Fourier transform infrared transmission spectra measurements are presented to characterize a multimode single-heterostructure oxide waveguide. An index contrast of $\Delta n = 0.06$ is observed between oxidized $x = 0.4$ and $x = 0.8$ $\text{Al}_x\text{Ga}_{1-x}\text{As}$ oxide layers. Absorption loss at $1.55\ \mu\text{m}$ is observed due to OH groups. Near-field images are presented showing waveguiding in a single-mode oxide double heterostructure. © 1999 American Institute of Physics. [S0003-6951(99)05446-7]

Since its discovery in 1990,¹ the wet thermal native oxide of the compound semiconductor AlGaAs has become an important material for optoelectronic and electronic devices.² These stable oxides have a low refractive index, good insulating properties, and are easily incorporated into heterostructures. AlGaAs oxides have previously been used in waveguiding applications for cladding layer index reduction,³ lateral confinement for buried strip waveguides,⁴ or to introduce birefringence into a mostly semiconductor core.⁵ In a recent study of the Al dependence of the refractive index in native oxides of $\text{Al}_x\text{Ga}_{1-x}\text{As}$ ($x = 0.3\text{--}0.97$),⁶ we observed suitable index variations (e.g., $\Delta n \geq 0.06$ for $x = 0.4\text{--}0.8$) to enable waveguiding by total internal reflection within native oxide heterostructures. In this letter, we demonstrate native oxide single- and double-heterostructure planar waveguides fabricated by fully oxidizing appropriate AlGaAs semiconductor heterostructures. By internally guiding light in oxide films, substantially larger interaction lengths allow the characterization of important absorption and scattering loss mechanisms not previously measurable via thin film transmission techniques. Understanding and minimizing such optical losses is particularly important for all applications in which the light directly passes through oxidized regions, as in birefringent waveguides,⁵ buried microlenses,⁷ and photonic lattices.⁸ We present here prism coupling characterization with fiber-probe loss measurements, secondary ion mass spectrometry (SIMS) depth profiles, and Fourier transform infrared (FTIR) transmission spectra on a multimode single-heterostructure (two-layer) waveguide. In addition, near-field images are shown which demonstrate waveguiding in a single-mode double-heterostructure (three-layer) oxidized waveguide.

Metalorganic chemical vapor deposition (MOCVD) is

used to grow two AlGaAs heterostructures on semi-insulating GaAs substrates: (1) a single heterostructure (SH) consisting of $1\ \mu\text{m}$ of $\text{Al}_{0.8}\text{Ga}_{0.2}\text{As}$ followed by $1.4\ \mu\text{m}$ of $\text{Al}_{0.4}\text{Ga}_{0.6}\text{As}$; and (2) a double heterostructure (DH) with $1\ \mu\text{m}$ of $\text{Al}_{0.8}\text{Ga}_{0.2}\text{As}$, $0.4\ \mu\text{m}$ of $\text{Al}_{0.4}\text{Ga}_{0.6}\text{As}$, and $0.6\ \mu\text{m}$ of $\text{Al}_{0.8}\text{Ga}_{0.2}\text{As}$. Both structures have $500\ \text{\AA}$ GaAs cap layers, and all layers are not intentionally doped. In each structure, the waveguide core is in the $\text{Al}_{0.4}\text{Ga}_{0.6}\text{As}$ layer which maintains a higher Ga content and refractive index relative to the $\text{Al}_{0.8}\text{Ga}_{0.2}\text{As}$ cladding layers after oxidation.⁶ The GaAs cap layer is removed in a 4:1 citric acid:30% H_2O_2 selective etch, and the heterostructures are thermally oxidized from the surface in water vapor as previously described⁶ at 493°C for 262 min (SH), and 492°C for 98 min (DH). The SH forms a multimode asymmetric waveguide where an upper cladding layer was omitted to allow prism coupling characterization of the indices and thicknesses of both layers. A prism coupling mode profile in Fig. 1 shows dips in the intensity of light reflected from the prism surface contacting the sample

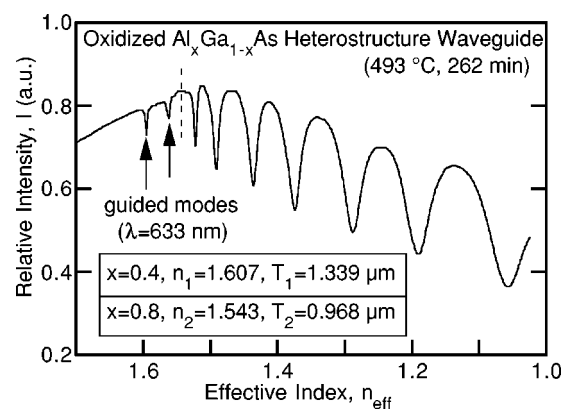


FIG. 1. Prism coupler mode profile for oxidized AlGaAs single-heterostructure planar waveguide. Two modes (marked with arrows) propagate in the upper, waveguiding layer. Inset shows measured indices (n_1 and n_2) and thicknesses (T_1 and T_2) of layers 1 and 2, respectively.

^{a)}Electronic mail: yluo@nd.edu

^{b)}Present address: EMCORE West, Albuquerque, New Mexico 87106.

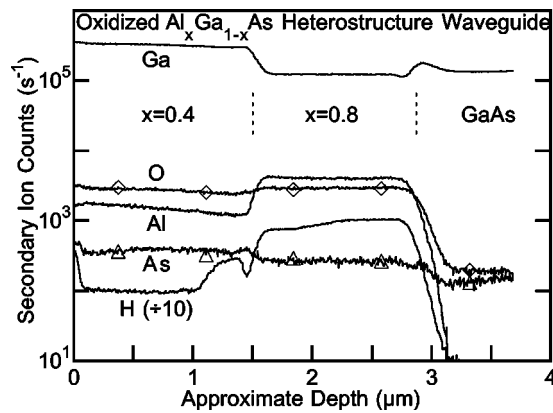


FIG. 2. Secondary ion mass spectrometry depth profiles for the oxide waveguide of Fig. 1. The oxide films are uniform, and the relative Al and Ga concentrations of the original $\text{Al}_{0.4}\text{Ga}_{0.6}\text{As}/\text{Al}_{0.8}\text{Ga}_{0.2}\text{As}$ single heterostructure are preserved after oxidation.

when the varying prism angle allows coupling into modes of the oxide films.⁹ Two modes with effective index $n_{\text{eff}} = \beta/k_0 = n_p \sin \theta_p = n_f \sin \theta_f$ exceeding the cladding layer index (marked by the vertical dashed line in Fig. 1) are guided by total internal reflection within the oxidized $\text{Al}_{0.4}\text{Ga}_{0.6}\text{As}$ upper layer. Here, the mode propagation constant $\beta = k \sin \theta_f$, where $k = 2\pi n_f/\lambda_0 = k_0 n_f$, $n_p = 1.9646$ is the prism index, $n_f = n_1$ is the top (guiding) film index, and θ_p and θ_f are the prism and film angles as defined in Fig. 3. Narrow dips are characteristic of guided modes, with broadening caused by propagation loss. The measured refractive indices (n_1, n_2) and thicknesses (T_1, T_2) of both layers are accurately determined from the relative mode positions, and are shown in the inset of Fig. 1. Index values are very close to those measured on single-layer films.⁶

Figure 2 shows SIMS depth profiles for Al, Ga, O, As, and H on the oxide SH of Fig. 1. Constituent concentrations are relative due to uncalibrated and matrix-dependent ion yield efficiencies. The H profile is shifted down one decade for clarity. The layer thicknesses and interface locations are approximate due to matrix-dependent sputtering rates and ion knock-in effects, and thus the actual interface abruptness cannot be deduced from Fig. 2. The profiles do demonstrate oxide uniformity and relative Al and Ga concentrations which are preserved in the two distinct $\text{Al}_x\text{Ga}_{1-x}\text{As}$ heterostructure regions, with no obvious layer interdiffusion during the oxidation process. The mode pattern in Fig. 1 does not contain the mode depth anomalies seen in initial studies.¹⁰ We attribute this to a more uniform distribution of As than observed previously,¹⁰ perhaps due to improved process control. A more uniform H distribution than shown in Ref. 10 may be due to a more complete moisture saturation of the hygroscopic films⁶ at the time of SIMS measurement. The presence of H may also indicate the existence of a hydroxide phase.⁶

Figure 3 shows propagation loss measurements at $\lambda_0 = 1.3$ and $1.55 \mu\text{m}$ for the first guided modes of the oxide SH of Figs. 1 and 2. The inset shows the prism coupling setup. A scanning fiber bundle is used to probe the spatial dependence of the scattered light intensity (directly proportional to the power propagating in the guided mode). Exponential fits over the range shown yield total attenuations of 3.0 cm^{-1}

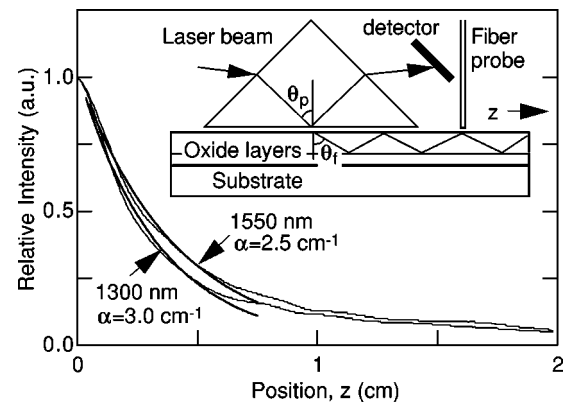


FIG. 3. Propagation loss at $\lambda_0 = 1.3$ and $1.55 \mu\text{m}$ for oxide waveguide of Figs. 1 and 2. The inset shows the prism coupler setup. The exponentially decaying guided mode power is directly proportional to the scattered light intensity collected by the scanned fiber-bundle probe.

(12.9 dB/cm) at $\lambda_0 = 1.3 \mu\text{m}$ and 2.5 cm^{-1} (10.7 dB/cm) at $1.55 \mu\text{m}$. The exponential tails (beyond $\sim 0.7 \text{ cm}$) contain random signal offsets due to stray background light and other spurious effects and are discarded for more reliable fitting. Estimated loss measurement accuracy is $\pm 20\%$. The attenuation ratio $\alpha(1.3 \mu\text{m})/\alpha(1.55 \mu\text{m})$ of 1.2 is less than the value of 2 predicted by Rayleigh's $1/\lambda_0^4$ law for volume scattering, or the value of 1.4 obtained by $1/\lambda_0^2$ theories for interface scattering.⁹ This suggests the presence of slightly greater loss due to absorption at 1.55 than $1.3 \mu\text{m}$. This can be attributed to the presence of hydroxyl (OH) groups remaining from the wet oxidation process, subsequent adsorption of moisture, and possible hydroxide phase components.⁶ The presence of OH groups in the oxide SH of Figs. 1–3 is confirmed by the FTIR transmission spectra shown in Fig. 4. Measurement at normal incidence results in Fabry–Perot resonances. A clear dip characteristic of OH vibration is observed at 3406 cm^{-1} ($\lambda_0 = 2.94 \mu\text{m}$). Similar results have been reported for oxidized AlAs.¹¹ The weak harmonic ($2\omega_0$) of the OH mode is still a source of loss at shorter wavelengths near $1.55 \mu\text{m}$. As seen by the marked positions of the 1.3 and $1.5 \mu\text{m}$ subharmonics (2×1.3 and $2 \times 1.55 \mu\text{m}$ in Fig. 4), the OH harmonic should result in loss in oxidized AlGaAs at 1.55 , but not $1.3 \mu\text{m}$. The losses measured on the waveguide in Fig. 3 would yield less than 0.1% absorption in normal incidence thin-film transmission measurements even on this relatively thick ($2.3 \mu\text{m}$) film, and are thus not evident at $1.55 \mu\text{m}$ (6452 cm^{-1}) and $1.3 \mu\text{m}$ (7692 cm^{-1}) in Fig. 4.

Loss measurements were also attempted at $\lambda_0 = 633$ and 830 nm , but the attenuation was too rapid for the technique of Fig. 3 which cannot reliably measure losses above about 7 cm^{-1} (30 dB/cm). We calculate that some of the loss at these wavelengths (~ 0.5 and $\sim 2.6 \text{ cm}^{-1}$, respectively) is attributed to absorption of the evanescent wave in the GaAs substrate, and could be avoided by use of a slightly thicker bottom cladding layer. Assuming no absorption loss at $1.3 \mu\text{m}$ according to the FTIR data of Fig. 4, the scattering loss at 830 nm should lie between 7.4 and 17.9 cm^{-1} , as projected using interface scattering theory⁹ and Rayleigh's law, respectively. It is well known that at a rough interface, scattering loss is higher for higher index contrasts. Lower scattering

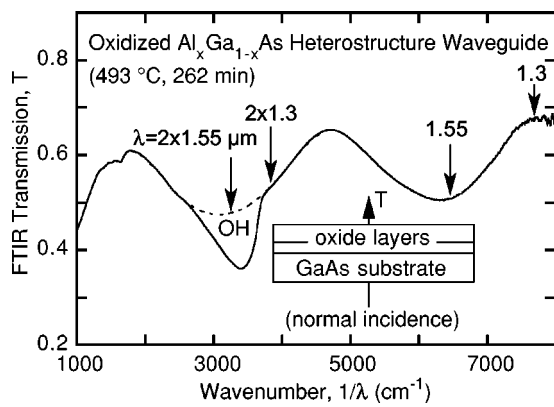


FIG. 4. Normal incidence Fourier transform infrared (FTIR) transmission spectrum of oxide waveguide of Figs. 1–3. Dip at 3400 cm^{-1} indicates absorption by OH groups. The dashed line indicates the interpolation of Fabry–Perot resonances.

tering losses should result from the addition of an oxide upper cladding layer.

We have also studied oxidation of an $\text{Al}_x\text{Ga}_{1-x}\text{As}$ DH waveguide, described above, designed to have a single mode both before and after oxidation. It might be desirable to integrate a transparent oxide waveguide with an active semiconductor laser or amplifier for integrated optics applications. One motivation is the possibility of realizing a monolithically pumped Er^{3+} -doped native oxide source or amplifier for $1.55\text{ }\mu\text{m}$ telecommunications applications, as AlGaAs native oxides appear to be better hosts than unoxidized semiconductors for optically active rare-earth dopants.¹² The TE-polarization near-field intensity profiles imaged on a linear charge-coupled device (CCD) array are shown in Fig. 5, demonstrating waveguiding in the DH before and after complete oxidation. The measured full width at half maximum (FWHM) at $\lambda_0 = 1.0\text{ }\mu\text{m}$ is $0.9\text{ }\mu\text{m}$ before and $2.1\text{ }\mu\text{m}$ after oxidation. For our imaging optic [$f = 3.1\text{ mm}$, 5 mm diameter (D) molded aspheric lens], the Airy diffraction “blur” radius at $\lambda_0 = 1.0\text{ }\mu\text{m}$ is $\rho = 1.22\lambda_0 f/D = 0.76\text{ }\mu\text{m}$ at the first zero ($0.32\text{ }\mu\text{m}$ at FWHM); diffraction effects thus prevent direct measurement

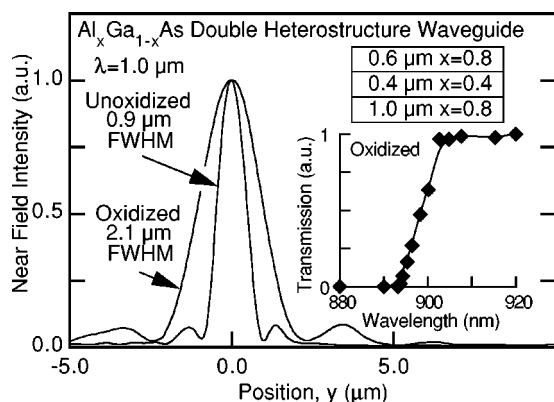


FIG. 5. Measured near-field intensity distributions for $\text{Al}_x\text{Ga}_{1-x}\text{As}$ DH single-mode waveguide before and after complete oxidation. The structure (shown in inset) was oxidized at $492\text{ }^\circ\text{C}$ for 98 min. An inset plot is shown of the relative oxide waveguide transmission near 900 nm .

of the actual mode dimensions. Simulated intensity FWHMs at $\lambda_0 = 1.0\text{ }\mu\text{m}$ are 0.34 and $0.73\text{ }\mu\text{m}$ using respective core/cladding indices for the semiconductor and oxide DH of $3.369/3.125$ and $1.607/1.543$. The inset in Fig. 5 shows that the transmission through the 1.8 mm long oxidized waveguide (measured using a tunable Ti:sapphire laser) abruptly cuts off below around 900 nm , the approximate start of the GaAs band edge absorption tail,¹³ indicating an inadequate lower cladding layer thickness to prevent substrate absorption. In comparison, the unoxidized waveguide has adequate mode confinement and is transparent to $<810\text{ nm}$ (the limits of our tuning range).

We have recently shown that a $\sim 2\times$ larger index contrast ($\Delta n \geq 0.12$) results if a small amount of oxygen ($\geq 300\text{ ppm}$) is present in the water vapor carrier gas (ultra-high purity N_2) during oxidation.⁶ This behavior is attributed to a transition from a hydroxide to a denser, more stable $(\text{Al}_x\text{Ga}_{1-x})_2\text{O}_3$ oxide phase, and promises to yield lower loss, higher confinement native oxide waveguides. Finally, we note that even with their rather large thicknesses (up to $2.3\text{ }\mu\text{m}$), our oxide films appear uniform, specular, and mechanically stable. Cleaving facets in the amorphous oxide DH is problematic, but large regions of apparently good facet quality are achieved by standard cleaving techniques. Cleaving after oxidation may be avoidable with an appropriate integration process.

In conclusion, we have demonstrated waveguiding within oxidized AlGaAs heterostructures and shown their utility for characterizing loss mechanisms not measurable by thin film transmission techniques. A slight absorption loss due to OH groups is present at $1.55\text{ }\mu\text{m}$. With further reductions in scattering and substrate absorption losses, practical transparent oxide waveguides, integratable with active semiconductor heterostructure devices, may potentially be realized.

This work was supported by NSF CAREER Award No. ECS-9502705.

- ¹J. M. Dallesasse, N. Holonyak, Jr., A. R. Sugg, T. A. Richard, and N. El-Zein, *Appl. Phys. Lett.* **57**, 2844 (1990).
- ²See K. D. Choquette, K. M. Geib, C. I. H. Ashby, R. D. Twisten, O. Blum, H. Q. Hou, D. M. Follstaedt, B. E. Hammons, D. Mathes, and R. Hull, *IEEE J. Sel. Top. Quantum Electron.* **3**, 916 (1997).
- ³A. Bek, A. Aydinli, J. G. Champlain, R. Naone, and N. Dagli, *IEEE Photonics Technol. Lett.* **11**, 436 (1999).
- ⁴M. R. Krames, E. I. Chen, N. Holonyak, Jr., A. C. Crook, T. A. De-Temple, and P.-A. Besse, *Appl. Phys. Lett.* **66**, 1912 (1995).
- ⁵A. Fiore, S. Janz, L. Delobel, P. Van der Meer, P. Bravetti, V. Berger, E. Rosencher, and J. Nagle, *Appl. Phys. Lett.* **72**, 2942 (1998).
- ⁶D. C. Hall, H. Wu, L. Kou, Y. Luo, R. J. Epstein, O. Blum, and H. Hou, *Appl. Phys. Lett.* **75**, 1110 (1999).
- ⁷O. Blum, K. L. Lear, H. Q. Hou, and M. E. Warren, *Electron. Lett.* **32**, 1406 (1996).
- ⁸P. W. Evans, J. J. Wierer, and N. Holonyak, Jr., *Appl. Phys. Lett.* **70**, 1119 (1997).
- ⁹P. K. Tien, *Appl. Opt.* **10**, 2395 (1971).
- ¹⁰Y. Luo, D. C. Hall, O. Blum, and H. Hou, in *Conference on Lasers and Electro-Optics, 1999*, OSA Technical Digest Series (Optical Society of America, Washington, D. C., 1999), pp. 139–140.
- ¹¹A. Fiore, V. Berger, E. Rosencher, N. Laurent, N. Vodjdani, and F. Nagle, *J. Nonlinear Opt. Phys. Mater.* **5**, 645 (1996).
- ¹²L. Kou, D. C. Hall, and H. Wu, *Appl. Phys. Lett.* **72**, 3411 (1998).
- ¹³R. G. Hunsperger, *Integrated Optics: Theory and Technology*, 2nd ed. (Springer, New York, 1985), p. 74.